Available online at www.sciencedirect.com
SCIENCE DIRECT®
Thermochimica Acta 414 (2004) 105–113
thermochimica acta
www.elsevier.com/locate/tca

Thermal and spectral studies of 5-(phenylazo)-2-thiohydantoin and 5-(2- hydroxyphenylazo)-2-thiohydantoin complexes of cobalt(II), nickel(II) and copper(II)

Samir S. Kandil*, Gad B. El-Hefnawy, Eman A. Baker

Chemistry Department, Faculty of Science, Tanta University, Tanta, Egypt

Received 25 March 2003; received in revised form 22 November 2003; accepted 22 November 2003

Abstract

Complexes of 5-(phenylazo)-2-thiohydantoin (L^1) and 5-(2-hydroxyphenylazo)-2-thiohydantoin (HL^2) with Co(II), Ni(II) and Cu(II) salts have been synthesised and characterized by elemental analysis, conductivity, magnetic susceptibility, UV-Vis, IR, ESR and TG studies. The magnetic and spectral data suggested octahedral geometry for $[L^1M(OAc)_2(H_2O)_2]\cdot xH_2O$ {M = Ni^{II} and Cu^{II}} and $[L^1CuCl_2(H_2O)]\cdot H_2O$ (dimeric form for the latter), trigonal bipyramidal geometry for $[L^2Co(OAc)(H_2O)]\cdot 2H_2O$, square pyramidal geometry for $[L^2Ni(OAc)(H_2O)]\cdot H_2O$ and square planar geometry for $[L^2CuCl]\cdot 2H_2O$. TG studies confirmed the chemical formulations of these complexes and showed that their thermal degradation takes place in three to five steps, depending on the type of the ligand and the geometry of the complex. The kinetic parameters (n, $E^{\#}$, A, $\Delta H^{\#}$, $\Delta S^{\#}$ and $\Delta G^{\#}$) of the thermal decomposition stages were computed using the Coats–Redfern and other standard equations and are discussed.

Keywords: Complexes; Synthesis; Thermal degradation; Thermogravimetry; Kinetics

1. Introduction

2-Thiohydantoins have been reported to be of biological importance as anticonvulsant, hypotonic and potential antitumor agents [1]. 2-Thiohydantions have been also used in other purposes, including textile printing [2], as catalysts for polymerization [3], in production of resins and plastics [4] and as qualitative reagents for detection of some metal ions upon complexation [5]. Transition metal ions have proven advantageous in improving stability, clarity and the brightness of the colour and effectiveness of the organic ligands in their applications. The present paper reports on the synthesis, spectral and thermal studies of some cobalt(II), nickel(II) and copper(II) complexes derived from 5-(phenylazo)-2-thiohydantoin and 5-(2-hydroxyphenylazo)-2-thiohydantoin, Scheme 1. The kinetic parameters n, $E^{\#}$ and A have been determined using Coats–Redfern method [6,7]. The other kinetic parameters $\Delta H^{\#}$, $\Delta S^{\#}$ and $\Delta G^{\#}$ have been computed using standard equations.

2. Experimental

2.1. Synthesis of the ligands

The ligands 5-(phenylazo)-2-thiohydantoin (L^1) and 5-(2-hydroxyphenylazo)-2-thiohydantoin (HL^2) were prepared and purified according to the methods reported in the literature [8,9].

2.2. Synthesis of metal complexes

Hot EtOH solution of L^1 or HL^2 (0.005 mol) and a hot H_2O-EtOH solution (50% (v/v)) of the metal(II) salts, namely, $NiCl_2\cdot 6H_2O$, $M(OAc)_2\cdot 4H_2O$ (M = Co^{II} or Ni^{II}), $CuCl_2\cdot 2H_2O$ or $Cu(OAc)_2\cdot H_2O$ (0.005 mol) were mixed and heated under reflux on water bath for 3 h with occasional stirring. In case of the acetate complexes, two to three drops of AcOH were added to the metal acetate solution. The reaction mixture was then concentrated by rotary evaporation under reduced pressure until the onset of precipitation of the products. The products were separated and washed successively with H_2O, warm EtOH and Et_2O, and dried in vacuo over anhydrous $CaCl_2$.

* Corresponding author.
E-mail address: kandilsamir@hotmail.com (S.S. Kandil).

0040-6031/$ – see front matter © 2003 Elsevier B.V. All rights reserved.
doi:10.1016/j.tca.2003.11.021

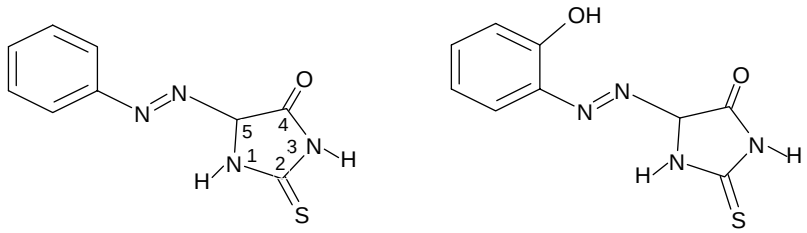

L^1 HL^2

Scheme 1. Structures of ligands L^1 and HL^2.

2.3. Analytical methods

Infrared spectra in the 4000–200 cm^{-1} range were recorded as KBr discs on a Perkin Elmer 683 spectrophotometer. Electronic spectra were recorded as nujol mulls on a Shimadzu 240 spectrophotometer. Magnetic susceptibilities were measured by the Gouy method. Diamagnetic corrections were made using Pascal's constants. Electron spin resonanace (ESR) spectra of powdered samples of the copper(II) complexes were recorded on a Jeol JEX-FE 2XG spectrometer using diphenyl-1-picrylhydrazone (DPPH) as standard ($g = 2.0036$). Thermogravimetric curves of the complexes were recorded on a Shimadzu DT-50 at heating rate of 10 °C min^{-1}, using 10–14 mg of powdered samples in nitrogen atmosphere. Microanalyses of C, H and N were performed at the Microanalytical center at Cairo University. The complexes were analyzed for their metal content by EDTA titration. Molar conductances in DMF were measured at room temperature on a Hanna 8733 conductivity meter.

3. Results and discussion

The metal complexes are microcrystalline, non-hygroscopic, partially soluble in most common organic solvents but entirely soluble in DMF and DMSO. The analytical data reveal 1:1 (metal:ligand) stoichiometry (Table 1). The molar conductance values fall in the 8−14 Ω^{-1} mol^{-1} cm^2 range, indicating the non-electrolytic nature of these complexes [10]. The magnetic moment values are in the range reported for high-spin Co(II) and Ni(II) complexes and magnetically dilute Cu(II) complexes containing an unpaired electron. The subnormal magnetic moment of $[L^1CuCl_2(H_2O)]\cdot H_2O$ indicates copper−copper interaction and suggests dimeric structure, presumably with chloride bridges [11].

3.1. Infrared spectra

The ligands L^1 and HL^2 show bands at 3290, 3180, 2890,1729/1715, 1424/1438 and 750 cm^{-1}, assigned to $\nu(N^1–H)$, $\nu(N^3–H)$, $\nu(C^5–H)$, $\nu(C=O)$ of 2-thiohydantoin moiety, $\nu(N=N)$ and thioamide IV modes, respectively [9,12]. The two strong bands at 1510 and 1330 cm^{-1} are assigned to the thioamide I and II modes, respectively [12]. The spectrum of HL^2 shows strong band at 1180 cm^{-1} assigned to the $\nu(C–O)$ mode of the phenol group. The absence of strong band at ∼2500 cm^{-1}, assignable to the $\nu(S–H)$ mode, indicate that both compounds exist in the thiono(C=S) form in the solid state. The IR spectra of the metal(II) complexes of L^1 and HL^2 show shifts to lower wavenumbers of the $\nu(C=O)$, $\nu(N=N)$ bands (by 34–46 and 13–22 cm^{-1}, respectively) and to higher wavenumbers of the $\nu(C–O)$ band (by 34–50 cm^{-1} in case of HL^2 complexes), compared to the values of the free ligands. These shifts suggest that the carbonyl–O of 2-thiohydantoin moiety, an azo–N and phenolic–O (in case of HL^2 complexes) atoms are involved in coordination to metal ions [13,14]. However, the thioamide I, II and IV bands show no significant wavenumber shifts in all complexes, indicating non-participation of the sulphur atom in bonding to metal ions. The acetate complexes show relatively broad bands at ∼1595 cm^{-1} which may be considered as overlap of the $\delta(N^1–H)$ and $\delta(N^3–H)$ modes with $\nu_{as}(OCO)$ of the acetate anions. On the other hand, the bands which appear in the 1361–1386 cm^{-1} region in the same complexes are assigned

Table 1
Analytical, magnetic and conductivity data of Co(II), Ni(II) and Cu(II) complexes with L^1 and HL^2

Complex (formula wt.)	Elemental analysis (%)				Molar conductance (Ω^{-1} mol^{-1} cm^2)	Magnetic moment (BM)
	C	H	N	M		
$[L^1CuCl_2(H_2O)]\cdot H_2O$ (390.5)	27.45 (27.65)	2.5 (3.1)	14.2 (14.3)	16.1 (16.3)	12	1.28
$[L^1Cu(OAc)_2(H_2O)_2]\cdot H_2O$ (455.5)	33.9 (34.2)	4.2 (4.4)	12.05 (12.3)	13.7 (13.9)	10	1.82
$[L^1Ni(OAc)_2(H_2O)_2]\cdot 2H_2O$ (468.7)	33.0 (33.3)	4.6 (4.7)	11.7 (11.9)	12.2 (12.5)	8	3.05
$[L^2CuCl]\cdot 2H_2O$ (370)	29.05 (29.3)	2.9 (3.0)	14.95 (15.1)	17.0 (17.2)	11	1.82
$[L^2Co(OAc)(H_2O)]\cdot 2H_2O$ (406.9)	32.1 (32.4)	3.6 (3.9)	13.6 (13.8)	14.35 (14.5)	14	4.53
$[L^2Ni(OAc)(H_2O)]\cdot 2H_2O$ (406.7)	32.2 (32.45)	3.7 (3.9)	13.5 (13.8)	14.05 (14.4)	9	2.84

to the ν_s(OCO) mode of the acetate groups. This affords separation wavenumber values Δ, ($\Delta = \nu_{as}$(OCO)–ν_s(OCO)), larger than 200 cm^{-1} for all the acetate complexes, characteristic of unidentate acetate anion [15]. In the chloro complexes, the bands that appear at 268 and 276 cm^{-1} in $[L^1CuCl_2(H_2O)]\cdot H_2O$ and $[L^2CuCl]\cdot 2H_2O$, respectively, are attributed to the ν(Cu–Cl) mode of terminal chloride ions and the shoulder at 238 cm^{-1} in the former one is due to the ν(Cu–Cl) mode of bridging chloride ions [16]. The broad nature of the bands appearing in the 650–500 cm^{-1} region may be attributed to overlapping of differnt stretching modes of the M–O bonds of carbonyl–O, water–O and acetate–O with the ligand bands.

The IR spectra of the complexes also show broad band around 3400 cm^{-1}, assignable to the two ν(N–H) modes overlapped with the stretching modes of water molecules.

3.2. UV-Vis spectra

The electronic spectrum of $[L^2Co(OAc)(H_2O)]\cdot 2H_2O$ shows d–d bands at 15,267 and 19,157 cm^{-1} which could be assigned to $^4A_2 \rightarrow {}^4A_2$(P) and $^4A_2 \rightarrow {}^4E_2$(P) transitions, respectively, similarly to trigonal bipyramidal cobalt(II) complexes of D_{3h} symmetry [17].

The visible spectrum of $[L^1Ni(OAc)_2(H_2O)_2]\cdot 2H_2O$ exhibits two bands at 16333 and 25907 cm^{-1}, attributable to $^3A_{2g}$(F) $\rightarrow {}^3T_{1g}$(F) (ν_2) and $^3A_{2g}$(F) $\rightarrow {}^3T_{1g}$(P) (ν_3) transitions, respectively, confirming octahedral geometry for this complex [18]. The spectrum of $[L^2Ni(OAc)(H_2O)]\cdot 2H_2O$ shows two absorption bands at 18,868 and 22,936 cm^{-1}, characteristic of high-spin five coordinate nickel(II) complexes [18] and could be assigned to $^3B_{1g} \rightarrow {}^3A_{2g}$(P) and $^3B_{1g} \rightarrow {}^3E_g$(P), respectively, of square pyramidal environment with D_{4h} microsymmetry.

The electronic spectra of $[L^1CuCl_2(H_2O)]\cdot H_2O$, $[L^1Cu(OAc)_2(H_2O)_2]\cdot H_2O$ exhibit a relatively broad band of low intensity at 16103 and 15873 cm^{-1}, respectively, assigned to the superimposed $^2B_{1g} \rightarrow {}^2B_{2g} + {}^2E_g + {}^2A_{1g}$ transitions, suggesting distorted octahedral structure for both complexes. The spectrum of $[L^2CuCl]\cdot 2H_2O$ displays a broad band at 15038 cm^{-1}, assignable to $^2B_{1g} \rightarrow {}^2A_{1g}$ transition in D_{4h} microsymmetry, which is consistent with square planar geometry [17].

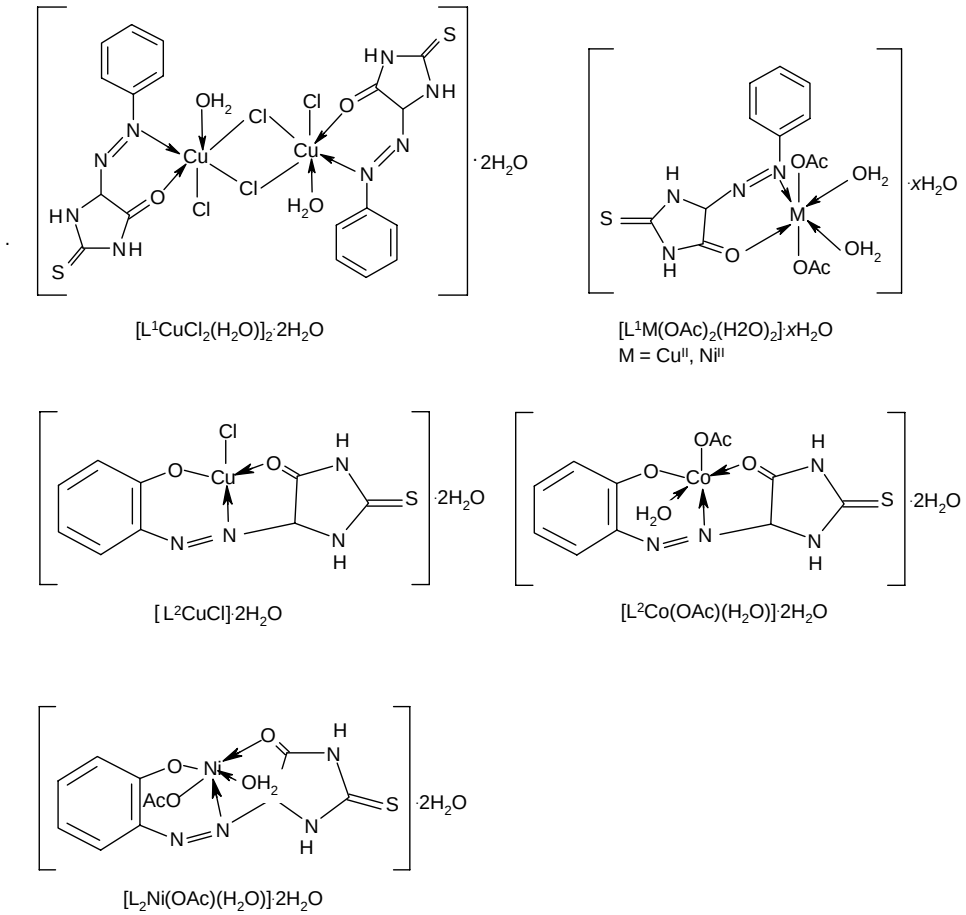

Scheme 2. Proposed structures of L^1 and HL^2 complexes.

3.3. Electron spin resonance spectra

The ESR spectra of $[L^1Cu(OAc)_2(H_2O)_2]\cdot H_2O$ and $[L^1CuCl_2(H_2O)]\cdot H_2O$ exhibit axial signals with g values of $g_{\parallel} = 2.285$ and 2.23, $g_{\perp} = 2.07$ and 2.065, respectively, fitted using the procedure given by Hathaway and Billing [19]. The fact that $g_{\parallel} > g_{\perp} > 2.0$ suggests an elongated octahedral geometry for the two complexes and that the unpaired electron is mainly in the $d_{x^2-y^2}$ orbital, with possibly some d_{z^2} character due to the low symmetry [20]. The spectrum of $[L^1CuCl_2(H_2O)]\cdot H_2O$ shows an additional, weak, half-field signal at 1587 G, due to $\Delta M_s = \pm 2$ transition, characteristic of magnetic interaction between copper centers [21], which is further supported by the subnormal magnetic moment (1.28 BM/Cu atom) of this complex. The complex $[L^2CuCl]\cdot 2H_2O$ gives an isotropic signal at $g = 2.12$, in accordance with square-planar geometry [17].

Based on the foregoing observations from elemental analysis, conductivity, magnetic moment and spectral studies, the following tentative structures, Scheme 2, are proposed for the present complexes.

3.4. Thermal analysis

The stages of decomposition, temperature range, decomposition product loss as well as the found and calculated weight loss percentages of the complexes are given in Table 2. The TG curve of $[L^1CuCl_2(H_2O)]\cdot H_2O$, Fig. 1, shows weight losses of 4.55 and 4.3% in temperature ranges 27–101 and 101–176 °C, corresponding to a loss of one water lattice molecule and one coordinated water molecule, respectively. $[L^2CuCl]\cdot 2H_2O$ shows a weight loss of 10.0% in the temperature range 27–112 °C which corresponds to volatilisation of two lattice water molecules. The next decomposition step of the two complexes, in the 176–392 °C range, brings weight loss of about 38.54 and 40.25% which correlate with elimination of $1/2Cl_2$ and decomposition of the 2-thiohydantoin fragment. The remaining of ligand L^1 (phenylazo moiety) is lost in the 382–637 °C range of the two complexes with elimination of another $1/2Cl_2$ in case of $[L^1CuCl_2(H_2O)]\cdot H_2O$. The elimination of the chlorides in two steps supports the presence of terminal and bridging chloride ions in this complex. There is no further mass loss beyond 637 and 607 °C for $[L^1CuCl_2(H_2O)]\cdot H_2O$ and

Table 2
Thermal behaviour of metal complexes of 5-(phenylazo)-2-thiohydantoin, L^1 and 5-(2-hydroxyphenylazo)-2-thiohydantoin HL^2

Compound (molecular weight)	DTG peak (°C)	Temperature range (°C)	Decomposition product lost (formula wt.)	Wt. (%) found (calculated)
$[L^1CuCl_2(H_2O)]\cdot H_2O$ (390.5)	72	27–101	$1H_2O$ (18)	4.3 (4.6)
	139	101–176	$1H_2O$ (18)	4.3 (4.6)
	352	176–382	$1/2\ Cl_2 + C_3H_3N_2OS$ (150.5)	38.45 (38.5)
	557	382–632	$1/2\ Cl_2 + C_6H_5N_2$ (140.5)	35.5 (36.0)
		632–800	Residue; Cu metal (63.5)	17.2 (16.3)
$[L^1Cu(OAc)_2(H_2O)_2]\cdot H_2O$ (455.5)	73	25–100	$1H_2O$ (18)	4.0 (3.95)
	176	100–236	$2H_2O$ (36)	7.7 (7.9)
	347, 450	236–481	$(CH_3)_2CO + C_3H_3N_2OS$ (173)	37.8 (38.0)
	588	481–640	$C_6H_5N_2$ (105)	22.8 (23.05)
	725	640–760	CO_2 (44)	9.6 (9.85)
		760–800	Residue; CuO (79.5)	18.1 (17.45)
$[L^1Ni(OAc)_2(H_2O)_2]\cdot 2H_2O$ (468.7)	75.5	27–102	$2H_2O$ (36)	7.5 (7.7)
	190	102–234	$2H_2O$ (36)	7.6 (7.7)
	352	234–425	$(CH_3)_2CO + C_3H_3N_2OS$ (173)	36.6 (36.9)
	526	425–570	$C_6H_5N_2$ (105)	22.3 (22.4)
	675.5	570–743	CO_2 (44)	9.2 (9.4)
		743–800	Residue; NiO (74.7)	16.1 (15.9)
$[L^2CuCl]\cdot 2H_2O$ (370)	81	35–112	$2H_2O$ (18)	10.0 (9.7)
	310	112–392	$1/2\ Cl_2 + C_3H_3N_2OS$ (150.5)	40.25 (40.7)
	488	392–608	$C_6H_4N_2$ (104)	28.3 (28.1)
		608–800	Residue; CuO (79.5)	22.45 (21.5)
$[L^2Ni(OAc)(H_2O)]\cdot 2H_2O$ (406.7)	77	31–124	$2H_2O$ (36)	8.7 (8.85)
	180	124–188	$1H_2O$ (18)	4.5 (4.4)
	400	188–515	$C_3H_3N_2OS + C_6H_4N_2$ (218)	55.0 (53.6)
	575	515–612	OAc (59)	13.8 (14.5)
		612–800	Residue; NiO (74.7)	17.9 (18.4)
$[L^2Co(OAc)(H_2O)]\cdot 2H_2O$ (406.9)	80	36–129	$2H_2O$ (36)	8.7 (8.8)
	200	129–225	$1H_2O$ (18)	4.85 (4.4)
	320	225–385	$C_3H_3N_2OS$ (114)	28.8 (28.0)
	519	385–625	$C_6H_4N_2 + OAc$ (163)	38.8 (40.06)
		625–800	Residue; CoO (74.7)	19.0 (18.75)

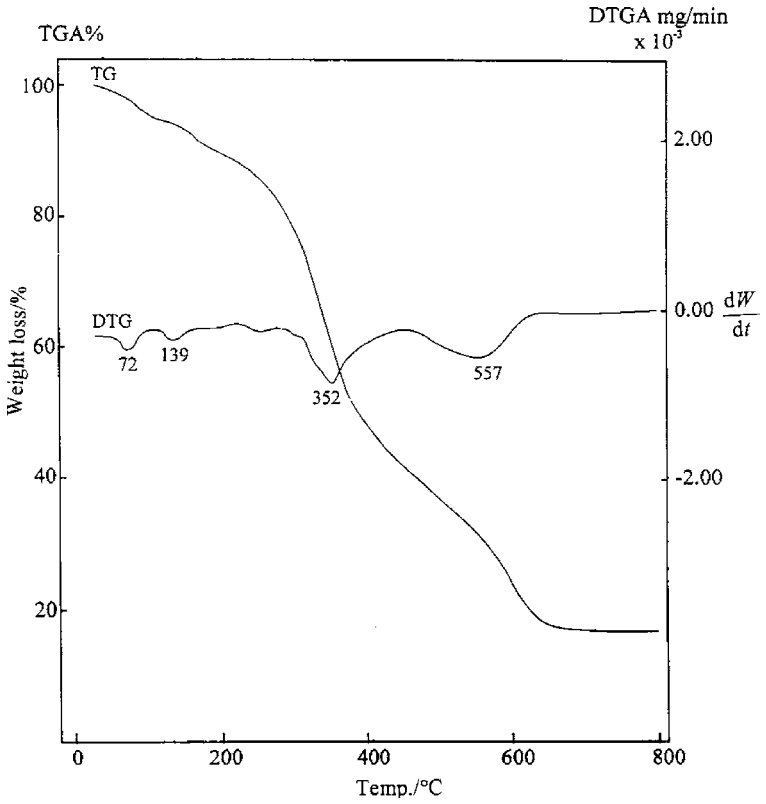

Fig. 1. TG and DTG curves of $[L^1CuCl_2(H_2O)]\cdot H_2O$.

$[L^2CuCl]\cdot 2H_2O$; a plateau is obtained which corresponds to the fomation of Cu and CuO, respectively.

The thermal decomposition curves of the $[L^1M(OAc)_2(H_2O)_2]\cdot xH_2O$, M = Ni^{II} and Cu^{II} (Fig. 2 as a representative example) show similar sequence of five decomposition steps which could be correlated with elimination of the following species:

(i) Lattice water molecules in the 25–120 °C range.
(ii) Coordinated water molecules in the100–236 °C range.
(iii) 2-Thiohydantoin moiety and acetone (resulting from decomposition of the two acetate groups) in the 234–481 °C range.
(iv) Phenylazo fragment ($C_6H_4N_2$) in the 425–640 °C range.
(v) Carbon dioxide in the 570–760 °C range.

The TG curves of $[L^2M(OAc)(H_2O)]\cdot xH_2O$, {M = Co^{II} and Ni^{II}}, Fig. 3, show four steps. In the first step, loss of lattice water occurs in the 31–129 °C range. The second step, 124–225 °C, represents the loss of coordinated water. In the case of the Co^{II} complex, the decomposition of 2-thiohydantoin occurs in a separate third step in the range 225–385 °C whereas in the case of the Ni^{II} complex, this step is overlapped with decomposition of phenylazo moiety in the temperature range 188–515 °C on the TG curve. For the Co^{II} complex the fourth step, in the range 385–625 °C, represents decomposition of the phenylazo moiety and the acetate group and for the Ni^{II} complex in the range 515–612 °C it represents loss of acetate.

In order to assess the influences of the structural properties of the ligand and the type of the metal on the thermal behaviour of the complexes, the order, *n*, and the heat of activation $E^{\#}$ of the various decomposition stages were determined from the TG and DTG themograms using the Coats–Redfern equations in the following form:

$$\ln\left[\frac{1-(1-\alpha)^{1-n}}{(1-n)T^2}\right] = \frac{M}{T} + B \quad \text{for } n \neq 1 \tag{1}$$

$$\ln\left[\frac{-\ln(1-\alpha)}{T^2}\right] = \frac{M}{T} + B \quad \text{for } n = 1 \tag{2}$$

where $M = -E^{\#}/R$ and $B = \ln AR/\Phi E^{\#}$; $E^{\#}$, R, A and Φ are the heat of activation, the universal gas constant, pre-exponential factor and heating rate, respectively.

The correlation coefficient, *r*, was computed using the least squares method for different values of *n*, by plotting the left-hand side of the Eqs. (1) and (2) versus 1000/*T*, Figs. 4–6. The *n* value which gave the best fit ($r \cong 1$) was chosen as the order parameter for the decomposition stage of interest. From the intercept and linear slope of such stage, the *A* and $E^{\#}$ values were determined,. The other kinetic parameters, $\Delta H^{\#}$, $\Delta S^{\#}$ and $\Delta G^{\#}$ were computed using the relationships: $\Delta H^{\#} = E^{\#} - RT$, $\Delta S^{\#} = R[\ln(Ah/kT) - 1]$ and $\Delta G^{\#} = \Delta H^{\#} - T\Delta S^{\#}$, where *k* is the Boltzmann's constant

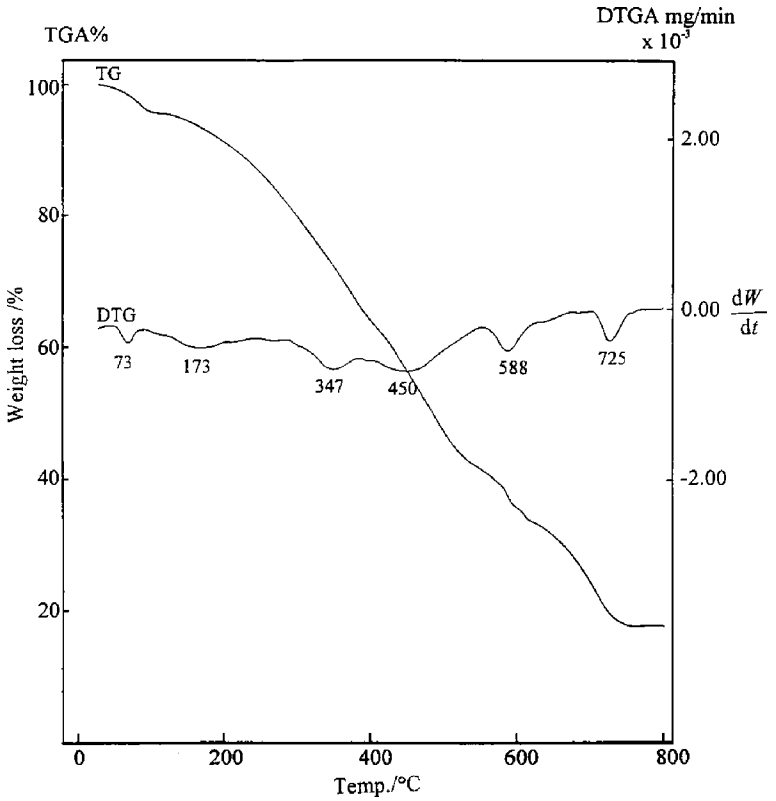

Fig. 2. TG and DTG curves of $[L^1Cu(OAc)_2(H_2O)_2]\cdot H_2O$.

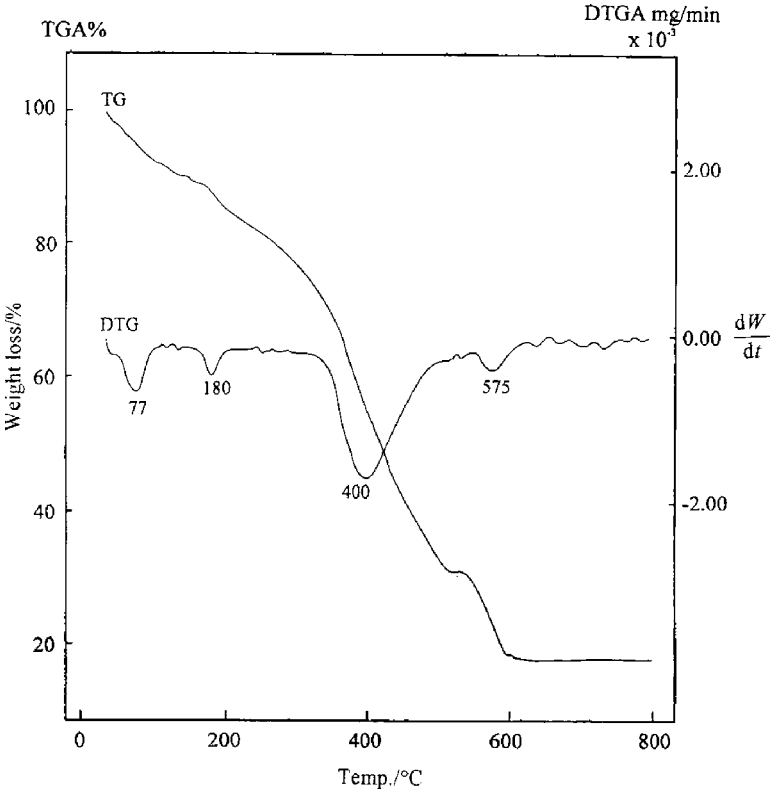

Fig. 3. TG and DTG curves of $[L^2Ni(OAc)(H_2O)]\cdot 2H_2O$.

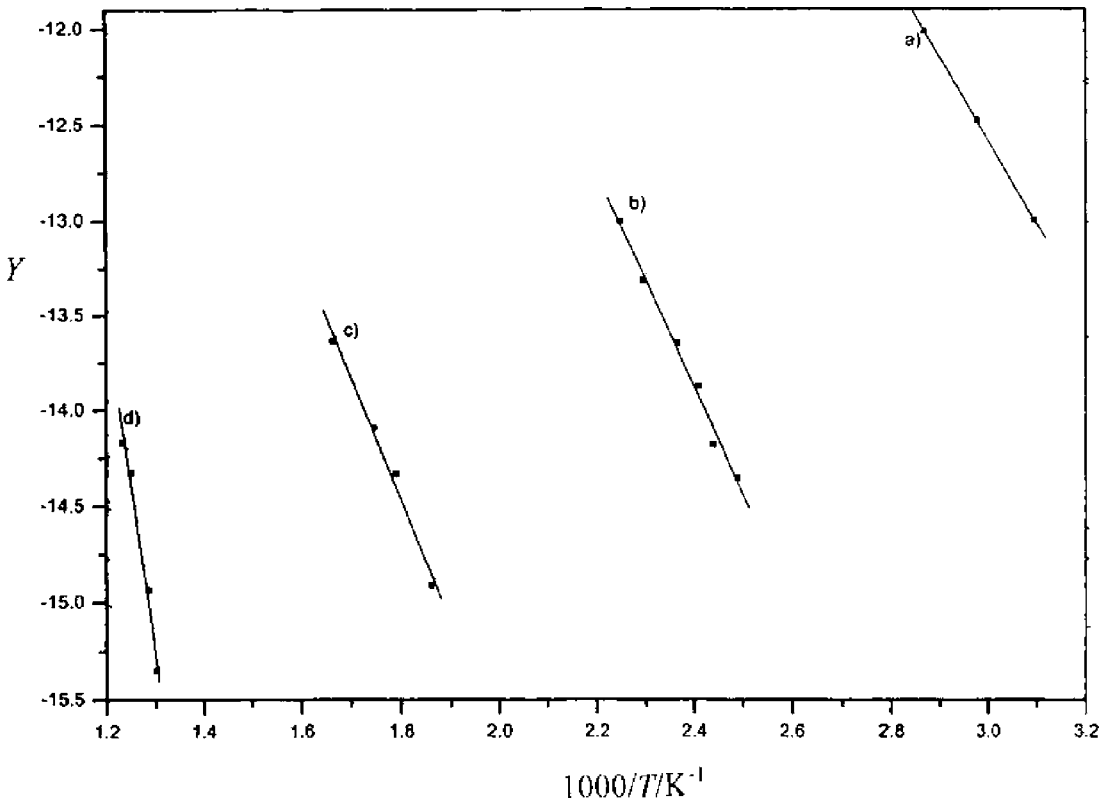

Fig. 4. Coast–Redfern plots for $[L^1CuCl_2(H_2O)]\cdot H_2O$: (a) first step; (b) second step; (c) third step; (d) fourth step; where $Y = [1-(1-\alpha)^{1-n}/(1-n)T^2]$ for $n \neq 1$, or $Y = [-\ln(1-\alpha)/T^2]$ for $n = 1$.

Table 3
Temperature of decomposition, order and activation parameters[a] of L^1 and HL^2 metal complexes

Complex	Step	T (K)	n	A^a	$E^{\#b}$	$\Delta H^{\#b}$	$\Delta S^{\#c}$	$\Delta G^{\#b}$
$[L^1CuCl_2(H_2O)]\cdot H_2O$	1st	345	0	20529.13	44.16	41.27	−0.164	97.85
	2nd	412	1	73.7	36.70	33.27	−0.212	120.56
	3rd	625	0.33	10.3	42.67	37.45	−0.232	182.25
	4th	830	1	3.86	35.30	28.38	−0.242	229.41
$[L^1Cu(Oac)_2(H_2O)_2]\cdot H_2O$	1st	346	1	1352.89	36.12	33.23	−0.187	97.79
	2nd	446	1	901.44	47.32	43.59	−0.192	129.09
	3rd	671.5	1	69.52	53.11	47.51	−0.216	192.83
	4th	861	1	3.8×10^6	142.95	135.78	−0.128	245.80
$[L^1Ni(OAc)_2(H_2O)_2]\cdot 2H_2O$	1st	348.5	1	1106.55	37.05	34.15	−0.188	99.67
	2nd	463	0.66	60779	57.90	57.9	−0.157	130.60
	3rd	625	1	2986.96	63.49	63.49	−0.195	185.36
	4th	799	0	139605	109.54	109.54	−0.165	241.37
$[L^2CuCl]\cdot 2H_2O$	1st	352	1	1.03×10^9	72.97	70.03	−0.049	89.28
	2nd	583	1	13.6	39.98	35.11	−0.229	168.50
	3rd	761.5	1	12222.1	96.30	89.94	−0.174	222.80
$[L^2Co(Oac)(H_2O)]\cdot 2H_2O$	1st	354	1	2497.7	39.03	36.07	−0.181	100.3
	2nd	473	1	2.73×10^6	77.50	73.56	−0.126	132.90
	3rd	593	0	12.74	45.97	41.02	−0.229	177.10
	4th	792	0.66	3.49×10^5	114.445	107.83	−0.147	224.30
$[L^2Ni(OAc)(H_2O)]\cdot 2H_2O$	1st	350	1	65.12	27.34	25.02	−0.212	99.06
	2nd	453	0.66	4.3×10^5	68.79	65.01	−0.141	128.70
	3rd	673	0.66	0.88	35.83	30.21	−0.253	200.30
	4th	848	1	212.7	86.41	79.33	−0.21	257.40

[a] Unit of A is s^{-1}.
[b] Unit of $E^{\#}$, $\Delta H^{\#}$ and $\Delta G^{\#}$ is $kJ\,mol^{-1}$.
[c] Unit of $\Delta S^{\#}$ is $kJ\,mol^{-1}\,K^{-1}$.

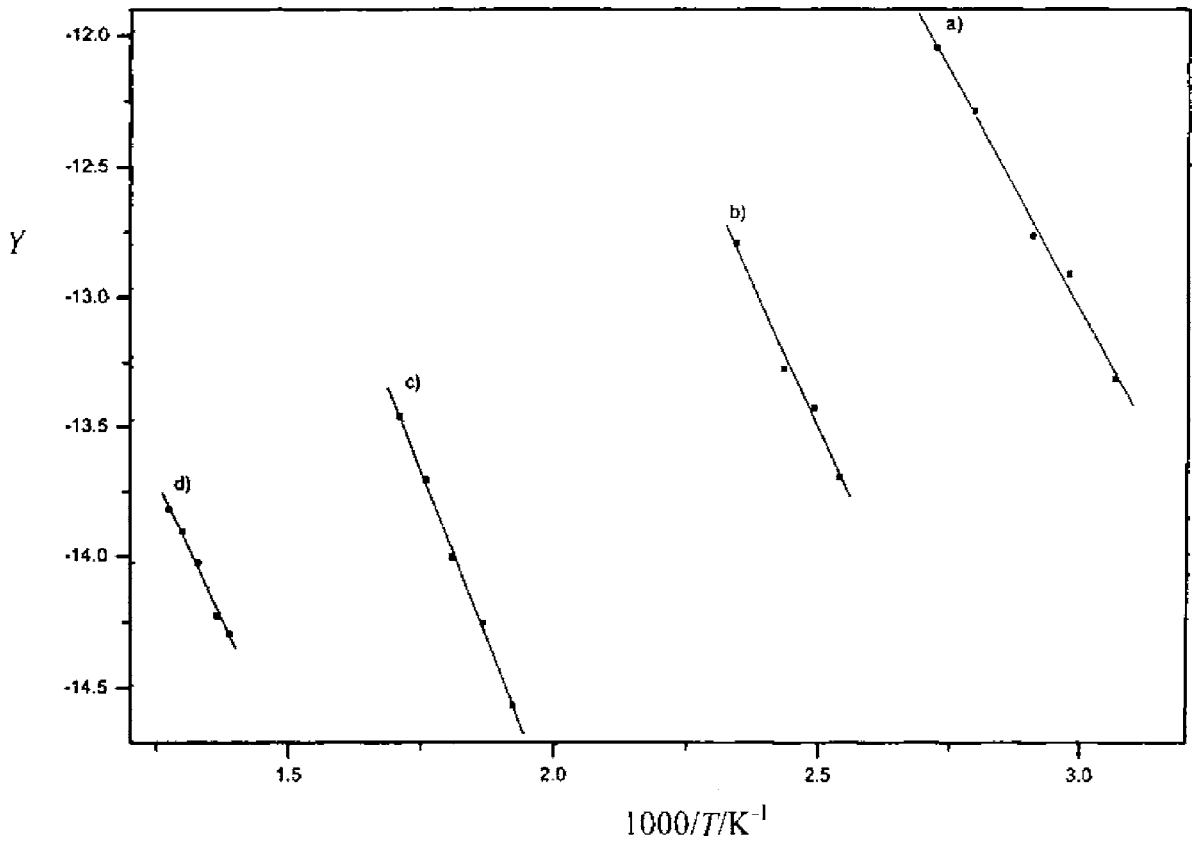

Fig. 5. Coats–Redfern plots for $[L^1Cu(OAc)_2(H_2O)_2]\cdot H_2O$.

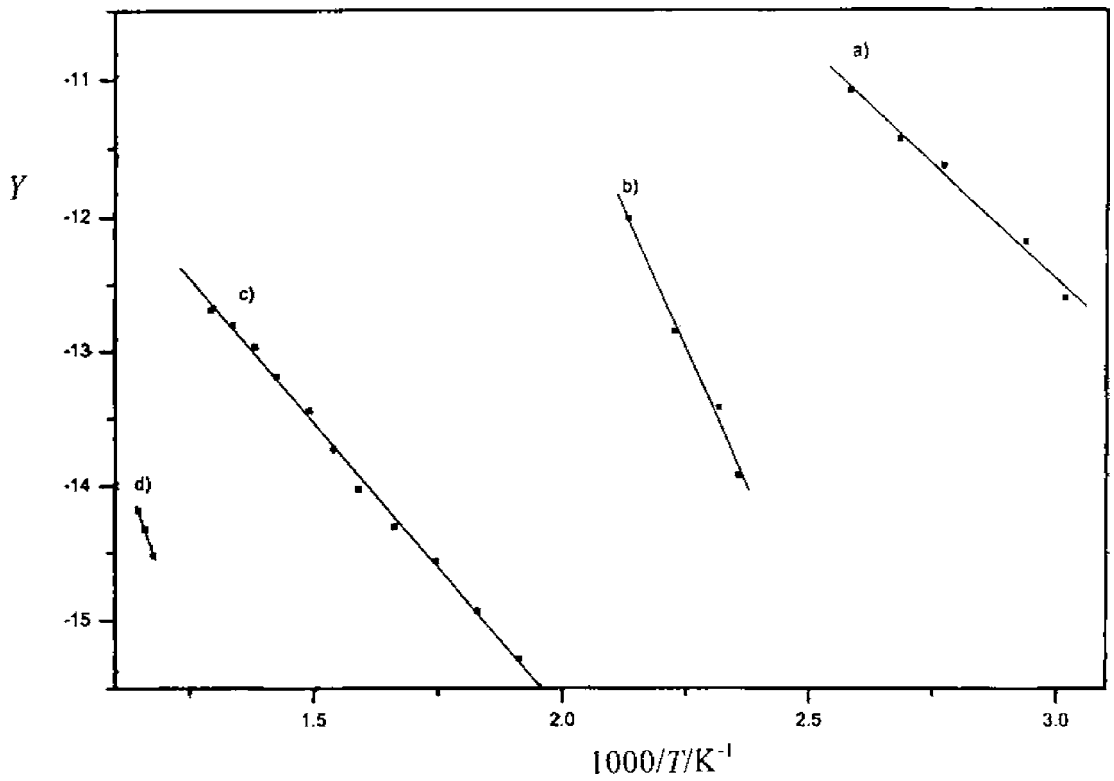

Fig. 6. Coats–Redfern plots for $[L^2Ni(OAc)(H_2O)]\cdot 2H_2O$.

and h is the Planck's constant. The kinetic parameters are listed in Table 3. The following remarks can be pointed out:

(i) The negative values of the activation entropies $\Delta S^{\#}$ indicate a more ordered activated complex than the reactants and/or the reactions are slow [22].

(ii) There are no obvious trends in the values of the heat of activation $E^{\#}$ or the activation enthalpies $\Delta H^{\#}$. However, the values of the activation energy $\Delta G^{\#}$ increases significantly for the subsequent decomposition stages of a given complex. This is due to increasing the values of $T\Delta S^{\#}$ significantly from one step to another which override the values of $\Delta H^{\#}$. Increasing the values of $\Delta G^{\#}$ for the subsequent steps of a given complex reflects that the rate of removal of the subsequent ligand will be lower than that of the precedent ligand [23,24]. This may be attributed to the structural rigidity of the remaining complex after the explusion of one and more ligands, as compared with the precedent complex, which requires more energy, $T\Delta S^{\#}$, for its rearrngement before undergoing any compositional change.

(iii) There is a conspicuous gap in the values of the heat of activation $E^{\#}$ and the enthalpy of activation $\Delta H^{\#}$ of volatilisation of lattice water between $[L^2CuCl]\cdot 2H_2O$ ($\Delta H^{\#} = 70.03\,kJ\,mol^{-1}$) and the two $[L^2M(OAc)(H_2O)]\cdot xH_2O$ ($\Delta H^{\#} = 36.07$ and $25.02\,kJ\,mol^{-1}$ for M = Co(II) and Ni(II), respectively). This may be attributed to the packing structure of $[L^2CuCl]\cdot 2H_2O$ which may allow stronger interactions of lattice water molecules in the crystal. However, the values of the $\Delta H^{\#}$ are compensated by the values of the entropies of activation, leading to almost the same values for the $\Delta G^{\#}$ ($89.28–100.30\,kJ\,mol^{-1}$) for this step of the three complexes.

(iv) The similar values of $\Delta G^{\#}$ for the decomposition steps involving the same decomposing species in the octahedral complexes $[L^1M(OAc)_2(H_2O)_2]\cdot xH_2O$ and to some extent in the structurally similar complexes $[L^2M(OAc)(H_2O)]\cdot xH_2O$, reveal that the mechanism of decomposition is the same and the effect of the ligands is more pronounced than that of the divalent metals.

(v) The reaction orders of the decomposition steps of the complexes are 1, 0.66, 0.33 and zero. It was emphasized that the reaction order of a solid-state decomposition has no intrinsic meaning, but is rather a mathematical smoothing device (parameter) [25].

References

[1] M.J. Gerhard (Nav, Acad. Anaapolis, MD) US NTIS, AD Rep. 1977, AD-AO 45373, Chemical Abstract, 88, 115462m, 1978, 81 pp.
[2] Société pour l'industrie chimique à Bâle, British Patent 330883 (1942).
[3] W.D. Stewart, US Patent 2430591 (1947).
[4] H.V. Wood, W.O. Drake, US Patent 3560470 (1971).
[5] N.M. Turkevich, U.F. Gerlich, Zh. Analit. Khim. 11 (1956) 180.
[6] A.W. Coats, J.P. Redfern, Nature 201 (1964) 68.
[7] N. Özpozan, H. Arslan, T. Özpozan, N. Özdes, N. Külcü, Thermochim. Acta 343 (2000) 127.
[8] V. Stella, T. Highnchi, J. Org. Chem. 38 (1937).
[9] S.S. Kandil, G.B. El-Hefnawy, E.A. Baker, A.Z. Abou El-Ezz, Transition Met. Chem. 28 (2003) 168.
[10] W.J. Geary, Coord. Chem. Rev. 7 (1971) 81.
[11] S.S. Kandil, G.Y. Ali, A. El-Dissouky, Transition Met. Chem. 27 (2002) 406, and refs. cited therein.
[12] R. Singh, S.K. Dikshit, Polyhedron 12 (1993) 759.
[13] D.C. Dash, F.M. Meher, P.C. Mohanty, J. Nanda, Indian J. Chem. 26A (1987) 698.
[14] N.V. Thakkar, R.M. Patil, Synth. React. Inorg. Met. Org. Chem. 30 (2000) 1159.
[15] G.B. Deacon, R.J. Phillips, Coord. Chem. Rev. 33 (1980) 227.
[16] K. Nakamoto, Infrared and Raman Spectra of Inorganic and Coordination Compounds, Wiley-Interscience, New York, 1986.
[17] A.B.P. Lever, Inorganic Electronic Spectroscopy, second ed., Elsevier, Amsterdam, 1984.
[18] L. Sacconi, Transition Met. Chem. 4 (1968) 227.
[19] B.J. Hathaway, D.E. Billing, Coord. Chem. Rev. 5 (1970) 143.
[20] G. Wilkinson, Comprehensive Coordination Chemistry, vol. 5, Pergmon Press, 1987, p. 663.
[21] K.K. Narang, V.P. Singh, Transition Met. Chem. 21 (1996) 507.
[22] A.A. Frost, R.G. Pearson, Kinetics and Mechanisms, Wiley, New York, 1961.
[23] P.B. Maravalli, T.R. Goudar, Thermochim. Acta 325 (1999) 35.
[24] K.K.M. Yusuff, R. Sreekala, Themochim. Acta 159 (1990) 357.
[25] D.B. Brown, E.G. Walton, J.C.S. Dalton (1980) 845.